



HAL
open science

A bifunctional triblock polynorbornene/carbon nanotube buckypaper bioelectrode for low-potential/high-current thionine-mediated glucose oxidation by FAD-GDH

Luminita Fritea, Andrew James Gross, Karine Gorgy, Rachel K. O'reilly, Alan Le Goff, Serge Cosnier

► To cite this version:

Luminita Fritea, Andrew James Gross, Karine Gorgy, Rachel K. O'reilly, Alan Le Goff, et al.. A bifunctional triblock polynorbornene/carbon nanotube buckypaper bioelectrode for low-potential/high-current thionine-mediated glucose oxidation by FAD-GDH. *Journal of Materials Chemistry A*, 2019, 7 (4), pp.1447-1450. 10.1039/C8TA10644D . hal-03014466

HAL Id: hal-03014466

<https://hal.science/hal-03014466>

Submitted on 19 Nov 2020

HAL is a multi-disciplinary open access archive for the deposit and dissemination of scientific research documents, whether they are published or not. The documents may come from teaching and research institutions in France or abroad, or from public or private research centers.

L'archive ouverte pluridisciplinaire **HAL**, est destinée au dépôt et à la diffusion de documents scientifiques de niveau recherche, publiés ou non, émanant des établissements d'enseignement et de recherche français ou étrangers, des laboratoires publics ou privés.



Journal Name

COMMUNICATION

A bifunctional triblock polynorbornene/carbon nanotube buckypaper bioelectrode for low-potential/high-current thionine-mediated glucose oxidation by FAD-GDH

Received 00th January 20xx,
Accepted 00th January 20xx

Luminita Fritea,^{a,b} Andrew J. Gross,^{a*} Karine Gorgy,^a Rachel K. O'Reilly,^c Alan Le Goff,^{a*} and Serge Cosnier,^{a*}

DOI: 10.1039/x0xx00000x

www.rsc.org/

We describe the fabrication of free-standing buckypaper bioelectrodes (BP) by co-immobilization of a FAD-dependent dehydrogenase and a thionine redox partner using either a pyreneNHS linker or a bifunctional triblock polynorbornene copolymer with pendant pyrene and NHS groups. While exhibiting excellent flexibility and conductivity, the BP bioelectrodes achieve high bioelectrocatalytic oxidation of glucose at onset potentials of -0.25V vs. Ag/AgCl and maximum current densities of 3.7 mA cm^{-2} at 50 mmol L^{-1} glucose.

Flavin adenine dinucleotide-dependent glucose dehydrogenase (FAD-GDH) is a glucose-oxidizing enzyme that has been proposed as a true alternative to the widely-investigated glucose oxidase for the catalytic oxidation of glucose in glucose biosensors and glucose biofuel cells.^{1,2} FAD-GDH is not inhibited by O_2 , nor does it produce H_2O_2 from the concomitant reduction of O_2 . This has the important advantage that FAD-GDH can efficiently operate in the presence of O_2 , which is of tremendous importance for glucose/ O_2 fuel cells.^{2,3} Furthermore, the presence of H_2O_2 is known to have deactivating effects on O_2 -reducing cathodes.² However, for the wiring of FAD-GDH at electrodes, a redox partner or a redox mediator is required in most cases. Different redox mediators have been studied so far for the wiring of FAD-GDH such as organic quinone derivatives,^{4–6} and osmium,^{1,7–9} ruthenium¹⁰ and metallocene complexes². These redox mediators have been mostly adsorbed either directly on electrodes, or covalently-attached to a polymer backbone then immobilized on the

electrode. Thionine, which features a phenothiazine core, has also been very recently envisioned as a low-potential redox mediator for FAD-GDH.^{5,11} In many of these examples, nanomaterials have been studied for the immobilization of the redox mediator and the wiring of FAD-GDH. In particular, multi-walled carbon nanotubes (MWCNTs) have proven to be a useful nanostructured platform for the co-immobilization of the enzyme and the redox mediator.^{12–16} Furthermore, the recent use of buckypapers (BPs) as CNT-based electrode supports has permitted the easy processability of flexible bioelectrodes for wearable and implantable fuel cell systems.¹⁷ In particular, we have recently developed the fabrication of freestanding buckypaper biocathodes based on functionalized-polynorbornene/MWCNT matrices.^{18,19} A multifunctional polynorbornene BP was used to bind 2-aminoanthraquinone and laccase from *Trametes versicolor* for bioelectrocatalytic oxygen reduction via the orientation of immobilized enzymes.¹⁸ The multifunctional polynorbornene copolymers were composed of a pyrene-based building block, for the reinforcement of the MWCNT matrix, and an NHS “grafting block”, for the binding of proteins.

In this work, we have developed the use of this type of multifunctional polynorbornene-based BP for the co-immobilization of both FAD-GDH and a redox mediator, thionine, for the MET-based oxidation of glucose. This free-standing BP was compared with a commercial MWCNT BP (from NanoTechLabs Inc.) modified via a previously-developed pyrene-NHS functionalization approach used for GDH wiring at glassy carbon-CNT electrodes²⁰. We developed and compared the fabrication processes for both types of MWCNT BPs towards the immobilization and wiring of FAD-GDH at flexible electrodes for low-potential mediated bioelectrocatalytic oxidation of glucose.

First, the preparation of the homemade free-standing BP was made according to our previously-described procedure with slight modification.¹⁸ In brief, a mixed suspension comprising 66 mg of MWCNTs and 16.5 mg of polynorbornene triblock

^a Département de Chimie Moléculaire, DCM, Univ. Grenoble Alpes, CNRS, 38000 Grenoble, France.

serge.cosnier@univ-grenoble-alpes.fr, alan.le-goff@univ-grenoble-alpes.fr, Andrew.gross@univ-grenoble-alpes.fr

^b Preclinical Disciplines Department, Faculty of Medicine and Pharmacy, University of Oradea, 10 Piata 1 Decembrie Street, 410073 Oradea, Romania.

^c School of Chemistry, University of Birmingham, Birmingham, UK.

Electronic Supplementary Information (ESI) available: [Materials and methods, NMR, IR, SEC, XPS, voltammetry and amperometric data]. See DOI: 10.1039/x0xx00000x

copolymer (Py₃₃-b-NHS₆₆-b-Py₃₃, 50 kg mol⁻¹) was prepared in 66 mL of DMF, filtered through a PTFE membrane under high vacuum, then washed, dried, and cut into 6 mm disk electrodes. The weight ratio of 20% polymer to 80% CNTs for the dispersion was chosen to give an optimal compromise between conductivity and mechanical stability.¹⁸ It is noted that the linear polymer comprises an ABA triblock sequence with an average of 50% of each of the pyrene and NHS ester groups. The polymer was characterised by IR, ¹HNMR and size exclusion chromatography (SEC) (Figure S1-S3). For preparation of the bioelectrode, both thionine and FAD-GDH were successively co-immobilized via coupling to the NHS groups (Figure 1). Thionine was immobilized in a first step in order to maximize its immobilization. The enzyme was then immobilized in a second step via unreacted NHS groups and physical adsorption. Control experiments showed that the chemical grafting initially of the enzyme then of the mediator gave electrodes that did not show catalysis. In order to study and compare a similar strategy, we explored the use of a commercial MWCNT BP, post-functionalized with 1-pyrenebutyric acid NHS ester (pyreneNHS), followed by the immobilization of thionine and then FAD-GDH (Figure 1).

insulating nature of the polymer, suggests improved interconnectivity between conductive CNTs in the homemade BP. The optical microscopy recorded at the visibly smoother sides of each BP revealed a more homogeneous surface structure at the polymer-based electrode (Figure 2b). PyreneNHS-based and polynorbornene-based BP electrodes were subsequently characterized by XPS after covalent immobilization of thionine (Figure S4 and S5). The XPS analysis confirms the presence of thionine at the surface of both types of BP, as indicated by the peaks at 164.2 and 165.4 eV, which are assigned to the S 2p_{1/2} and 2p_{3/2} binding energies, respectively. The element ratio N/S was calculated as 3.6 instead of 3 for pyreneNHS-based BP and 2.8 instead of 4 for polynorbornene-based BP. This indicates that pyreneNHS molecules are not fully functionalized by thionine in the pyreneNHS-based commercial BP while a relatively larger amount of non-specifically adsorbed thionine, entrapped in the copolymer, might account for the low N/S ratio observed for polynorbornene-based BP.

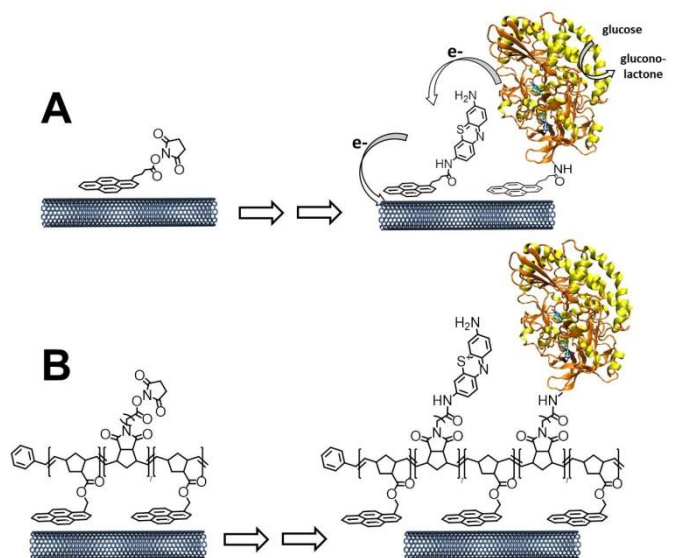


Figure 1. Schematic representation of the functionalization of MWCNT-based BP with (A) pyrene-NHS and (B) polynorbornene-pyrene-NHS polymer followed by the sequential immobilization of thionine and FAD-GDH

Characterization of buckypapers was done using laser scanning microscopy, conductivity measurements, X-ray photoelectron spectroscopy (XPS) and electrochemistry. Figure 2a shows the impressive flexibility of the polynorbornene-based BP. This is in contrast to the more fragile and less bendable commercial BP. The average conductivity (and thickness) for the pyreneNHS- and polynorbornene-based BPs are 1.8 S cm⁻¹ (270 μm) and 5.8 S cm⁻¹ (360 μm), respectively, based on four-point probe and Vernier caliper measurements at room temperature (average values obtained from 6 independent BP samples). The higher conductivity at the polynorbornene BP electrode, despite the

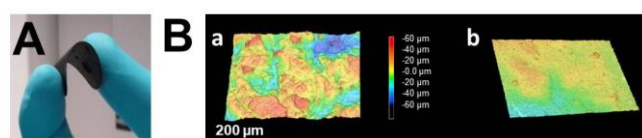


Figure 2. (A) Photograph of the flexible free-standing polynorbornene/MWCNT BP; (B) laser scanning microscopy image of the surface topography of (a) pyreneNHS BP and (b) polynorbornene BP

The redox properties of pyreneNHS-modified and polynorbornene-modified BP electrodes, after immobilization of thionine, were studied without glucose in pH 7 0.1 mol L⁻¹ PB at 25°C by cyclic voltammetry (CV, Figure 3).

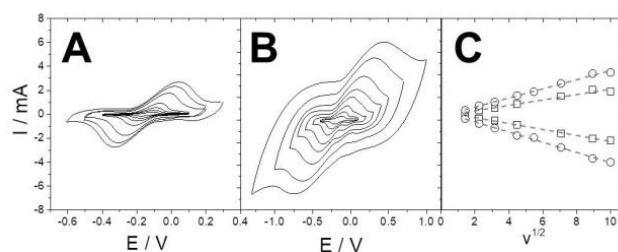


Figure 3. CV scans for (A) pyreneNHS-based BP and (B) polynorbornene-based BP at different scan rates: 2, 5, 10, 20, 30, 50, 80 and 100 mV s⁻¹ (0.1 M PB, pH 7, 25°C); (C) Evolution of oxidation and reduction peak current towards square root of scan rate for (□) pyreneNHS-based BP and (○) polynorbornene-based BP with immobilized thionine

A single reversible system is observed at $E_{1/2} = -0.14$ V vs. Ag/AgCl, corresponding to the electroactivity of thionine. The electroactivity of thionine at neutral pH corresponds to a 2 electron/1 proton process leading to leucothionine. Oxidation and reduction peak currents are highly stable upon multiple CV scans at both types of BP (Figure S6). Furthermore, a linear dependence of oxidative and reductive peak currents towards the square root of the scan rate is observed. The peak-to-peak separation is also > 59 mV for scan rates in the range 2-100 mV s⁻¹. This underlines that electron transfer is diffusion-controlled, as is commonly observed in redox hydrogels employed for MET-

based wiring of enzymes.^{21–25} By integration of the charge under the thionine redox system at low scan rate, a surface concentration of 0.16 nmol cm⁻² and 0.27 nmol cm⁻² was estimated for thionine immobilized on pyreneNHS-based BP and polynorborene-based BP, respectively. A higher amount of thionine at the surface of polynorborene-based BP likely arises from the higher number of available NHS groups, facilitated by the flexible NHS linker ($n = 7$), at the surface of the polymer-coated CNTs, as compared to the pyreneNHS-modified CNTs. This behaviour can be expected owing to the supramolecular nature of pi-stacking of pyrene molecules onto CNT sidewalls,²⁰ which is governed by a Langmuir isotherm and leads to an incomplete coverage of CNT sidewalls.

The bioelectrocatalytic properties of each of the functionalized BPs were studied in the presence of glucose (Figure 4). For both types of BPs, upon addition of 150 mmol L⁻¹ glucose, an electrocatalytic irreversible wave is observed with an onset potential of -0.25 V vs. Ag/AgCl. This confirms that MET is achieved between immobilized thionine and FAD-GDH. It is noteworthy that it is a gain of almost 100 mV in terms of overpotential for the MET wiring of FAD-GDH compared to an organic redox mediator such as phenanthrolinequinone, and a gain of around 250 mV compared to an osmium-based or ruthenium-based redox mediator.^{4,9,10} Maximum current densities of 3.03 mA cm⁻² and 1.98 mA cm⁻² were observed at 0.2 V for polynorborene-based BP and pyreneNHS-based BP, respectively.

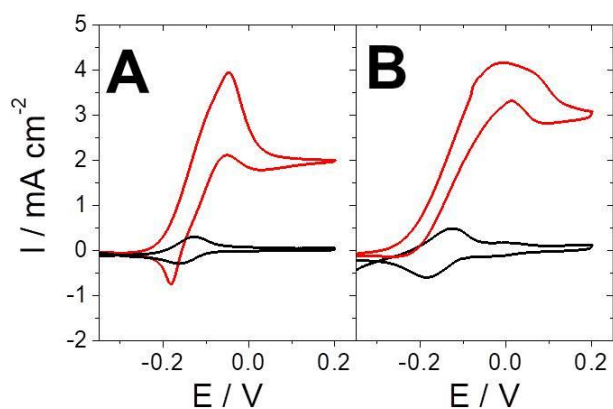


Figure 4. CV scans recorded before and after addition of 150 mmol L⁻¹ glucose for (A) pyreneNHS-based BP and (B) polynorborene-based BP with immobilized thionine and FAD-GDH (1 mV s⁻¹, 0.1 mol L⁻¹ PB, pH 7, 25°C).

Chronoamperometric measurements were performed at $E_p = 0.2$ V vs Ag/AgCl in the presence of increasing concentrations of glucose (Figure 5A).

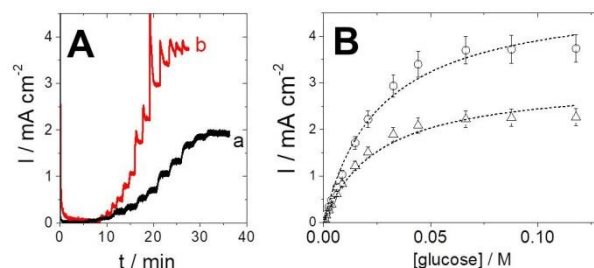


Figure 5. (A) Chronoamperometric measurements performed at $E_p = 0.2$ V for (a) pyreneNHS-based BP and (b) polynorborene-based BP with immobilized thionine and FAD-GDH after addition of successive amounts of glucose with stirring in 0.1 mol L⁻¹ PB pH 7, 25 °C; (B) Evolution of the current density with the glucose concentration accompanied with a fitting curve using a classic Michaelis-Mentens dependence. Error bars correspond to one standard deviation from at least two electrodes.

Both types of BP exhibit a typical Michaelis-Mentens dependence with a K_M value of 25 mmol L⁻¹ for both BPs (Figure 5B). Maximum current densities were obtained for homemade polynorborene-based BPs with 3.7 mA cm⁻² beyond 50 mmol L⁻¹ glucose. A linear region is observed between 0 and 15 mmol L⁻¹ glucose with sensitivity of 0.12 mA mol⁻¹ L cm⁻² ($R^2 = 0.999$) and 0.093 mA mol⁻¹ L cm⁻² ($R^2 = 0.982$) for polynorborene-based BP and pyreneNHS-based BP, respectively, accompanied with a limit of detection of 600 μ M (Figure S7). Furthermore, stability experiments examined by 30-min chronoamperometric measurements at 0.2 V vs Ag/AgCl show that polynorborene-based BP bioelectrodes retain 68% of their electrocatalytic activity after 7 days (Figure S8A) while pyreneNHS-based BPs exhibit 20% of their initial activity after 7 days (Figure S8B). The enhanced catalytic stability observed for the polynorborene-based electrode is attributed, at least in part, to improved enzyme stabilization via non-covalent enzyme entrapment in the polymer-CNT matrix. The stabilisation may be due to factors such as improved retention of the enzyme at the electrode and preservation of the enzyme's active conformation. The polymer-CNT matrix benefits from effective cross-linking, owing to the presence of multiple pyrene groups per polymer chain that can cross-link CNTs and thionine. In contrast, the BP electrode with pyrene-NHS cannot effectively cross-link. The cross-linked polynorborene-CNT electrode is therefore expected to be more robust than the pyrene-NHS electrode. Furthermore, the higher number of available NHS groups at the surface of the polynorborene BPs induces a higher number of thionine wired enzyme per surface unit as compared to the supramolecular pyrene-NHS modification, the later being a reversible phenomenon governed by Langmuir insotherm.²⁰ For comparison, FAD-GDH entrapped in osmium hydrogels at hierarchically structured porous electrodes exhibit maximum current densities of 100 mA cm⁻² (but at a much higher potential of 0.5 V vs. Ag/AgCl, with onset potentials of 0.0 V, and only under hydrodynamic conditions)⁹. For comparison, thionine and FAD-GDH adsorbed on gold nanoparticle-modified electrodes exhibit a maximum current density of 1.6 mA cm⁻² with an onset potential of -0.24 V¹¹. We recently reported a powerful catalytic glucose oxidation but with limited stability at a homemade BP electrode with adsorbed FAD-GDH and phenanthrolinequinone

which exhibited a maximum current density of 5.4 mA cm⁻² with onset potentials of -0.15 V⁴. The catalytic current of the phenanthroline quinone electrode was only around ca. 35% of its initial catalytic activity after 7 days, however, highlighting further beneficial performance of the polynorbornene-based thionine BP bioelectrode in terms of stability.

Conclusions

Here is described a performant biomaterial based on buckypapers for bioelectrocatalytic glucose oxidation via immobilization of both FAD-GDH enzyme and thionine redox mediator using an ABA triblock polynorbornene copolymer substituted with alternating pyrene and NHS groups. Compared to buckypaper prepared with the classical molecular linker, pyreneNHS, the buckypaper with the polynorbornene exhibited higher current densities of 3.7 mA cm⁻² at a lower potential with increased stability, flexibility and conductivity. The interest of using triblock polynorbornene copolymers for bioanode construction is therefore highlighted for the first time towards the goal of wearable and implantable bioelectrodes for biofuel cell and biosensor applications

Acknowledgments

This work was supported by the Labex ARCANÉ, CBH-EUR-GS (ANR-17-EURE-0003) and Campus France. The authors wish to acknowledge the support from the platform Chimie NanoBio ICMG FR 2607 (PCN-ICMG). The authors are grateful both to Yannig Nedellec, for conductivity and thickness measurements, and to Valerie Flaud from ICGM Montpellier for XPS characterization.

Notes and references

- M. N. Zafar, N. Beden, D. Leech, C. Sygmund, R. Ludwig and L. Gorton, *Anal. Bioanal. Chem.*, 2012, **402**, 2069–2077.
- R. D. Milton, F. Giroud, A. E. Thumser, S. D. Minter and R. C. T. Slade, *Phys. Chem. Chem. Phys.*, 2013, **15**, 19371–19379.
- R. D. Milton, F. Giroud, A. E. Thumser, S. D. Minter and R. C. T. Slade, *Chem. Commun.*, 2014, **50**, 94–96.
- A. J. Gross, X. Chen, F. Giroud, C. Abreu, A. Le Goff, M. Holzinger and S. Cosnier, *ACS Catal.*, 2017, **7**, 4408–4416.
- N. Tsuruoka, T. Sadakane, R. Hayashi and S. Tsujimura, *Int. J. Mol. Sci.*, 2017, **18**, 604.
- C. Hou, Q. Lang and A. Liu, *Electrochimica Acta*, 2016, **211**, 663–670.
- P. Pinyou, A. Ruff, S. Poeller, S. Ma, R. Ludwig and W. Schuhmann, *Chem.-Eur. J.*, 2016, **22**, 5319–5326.
- K. Murata, W. Akatsuka, T. Sadakane, A. Matsunaga and S. Tsujimura, *Electrochimica Acta*, 2014, **136**, 537–541.
- S. Tsujimura, K. Murata and W. Akatsuka, *J. Am. Chem. Soc.*, 2014, **136**, 14432–14437.
- R. Sakuta, K. Takeda, T. Ishida, K. Igarashi, M. Samejima, N. Nakamura and H. Ohno, *Electrochem. Commun.*, 2015, **56**, 75–78.
- A. Navaee and A. Salimi, *J. Electroanal. Chem.*, 2018, **815**, 105–113.
- S. Cosnier, M. Holzinger and A. Le Goff, *Front. Bioeng. Biotechnol.*, 2014, **2**, 45.
- S. Cosnier, A. J. Gross, A. Le Goff and M. Holzinger, *J. Power Sources*, 2016, **325**, 252–263.
- A. Le Goff, M. Holzinger and S. Cosnier, *Cell. Mol. Life Sci.*, 2015, **72**, 941–952.
- M. Holzinger, A. Le Goff and S. Cosnier, *Electrochimica Acta*, 2012, **82**, 179–190.
- M. Rasmussen, S. Abdellaoui and S. D. Minter, *Biosens. Bioelectron.*, 2016, **76**, 91–102.
- A. J. Gross, M. Holzinger and S. Cosnier, *Energy Environ. Sci.*, 2018, **11**, 1670–1687.
- A. J. Gross, M. P. Robin, Y. Nedellec, R. K. O'Reilly, D. Shan and S. Cosnier, *Carbon*, 2016, **107**, 542–547.
- S. Cosnier, R. Haddad, D. Moatsou and R. K. O'Reilly, *Carbon*, 2015, **93**, 713–718.
- B. Reuillard, A. Le Goff and S. Cosnier, *Chem. Commun.*, 2014, **50**, 11731–11734.
- A. Aoki and A. Heller, 1993, 11014–11019.
- F. Mao, N. Mano and A. Heller, *J. Am. Chem. Soc.*, 2003, **125**, 4951–4957.
- N. Plumeré, O. Rüdiger, A. A. Oughli, R. Williams, J. Vivekananthan, S. Pöller, W. Schuhmann and W. Lubitz, *Nat. Chem.*, 2014, **6**, 822–827.
- S. Rengaraj, R. Haddad, E. Lojou, N. Duraffourg, M. Holzinger, A. Le Goff and V. Forge, *Angew. Chem. Int. Ed.*, 2017, **56**, 7774–7778.
- L. Altamura, C. Horvath, S. Rengaraj, A. Rongier, K. Elouarzaki, C. Gondran, A. L. B. Maçon, C. Vendrely, V. Bouchiat, M. Fontecave, D. Mariolle, P. Rannou, A. Le Goff, N. Duraffourg, M. Holzinger and V. Forge, *Nat. Chem.*, 2017, **9**, 157–163.